SAND--98-1003

SANDIA REPORT

SAND98–1003 • UC–722
Unlimited Release
Printed April 1998

Analysis in Support of Storage of Residues in the Pipe Overpack Container

J. S. Ludwigsen, D. J. Ammerman, H. D. Radloff

Prepared by
Sandia National Laboratories
Albuquerque, New Mexico 87185 and Livermore, California 94550

Sandia is a multiprogram laboratory operated by Sandia Corporation, a Lockheed Martin Company, for the United States Department of Energy under Contract DE-AC04-94AL85000.

Sandia National Laboratories

Issued by Sandia National Laboratories, operated for the United States Department of Energy by Sandia Corporation.

Available to DOE and DOE contractors from
Office of Scientific and Technical Information
P.O. Box 62
Oak Ridge, TN 37831

Prices available from (615) 576-8401, FTS 626-8401

Available to the public from
National Technical Information Service
U.S. Department of Commerce
5285 Port Royal Rd
Springfield, VA 22161

NTIS price codes
Printed copy: A03
Microfiche copy: A01

SAND98-1003
Unlimited Release
Printed April 1998

Distribution
Category UC-722

Analysis in Support of Storage of Residues in the Pipe Overpack Container

J. S. Ludwigsen, D. J. Ammerman, and H. D. Radloff
Transportation Systems Department
Sandia National Laboratories
P.O. Box 5800
Albuquerque, NM 87185-0717

Abstract

The disposition of the large back-log of plutonium residues at the Rocky Flats Environmental Technology Site (Rocky Flats) will require interim storage and subsequent shipment to a waste repository. Current plans call for disposal at the Waste Isolation Pilot Plant (WIPP) and the transportation to WIPP in the TRUPACT-II. The transportation phase will require the residues to be packaged in a container that is more robust than a standard 55-gallon waste drum. Rocky Flats has designed the Pipe Overpack Container to meet this need. The potential for damage to this container during on-site storage in unhardened structures for several hypothetical accident scenarios has been addressed using finite element calculations. This report will describe the initial conditions and assumptions for these analyses and the predicted response of the container.

Table of Contents

List of Figures 3
List of Tables 4
1. Introduction 5
2. Background Information 5
3. Forklift Tine Analyses 6
   3.1. Finite element modeling 7
   3.2. 12 inch Diameter Inner Container Results 10
   3.3. 6 inch Diameter Inner Container Results 13
   3.4. Summary of Forklift Tine Impact Analyses 17
4. Roof Collapse Analyses 18
   4.1. Top Impact Results 19
   4.2. Side Impact Results 21
   4.3. Edge Impact Results 25
   4.4. Summary of Roof Collapse Analyses 25
5. Conclusions 31
6. References 31

DISCLAIMER

List of Figures

1. Diagram of the Pipe Overpack Container....6
2. Finite element model of the Pipe Overpack Container with 12 inch inner pipe....10
3. Finite element mesh of the tine impacting the outer drum wall....11
4. Mesh showing tine piercing the drum wall....11
5. View of the drum wall with failed elements removed from the mesh....12
6. Mesh showing the position of the tine at the beginning of the second portion of the analysis....12
7. Deformed shape of the model after tine impact....13
8. Equivalent plastic strain in the pipe wall after failed elements have been removed....14
9. Mesh used in the analysis of the 6 inch pipe overpack container....14
10. Deformed shape of the 6 inch pipe overpack container....15
11. Equivalent plastic strains in the pipe wall after impact....16
12. Overhead view of the impact between the tine and the 6 inch diameter inner cylinder at times of 0, 0.018, and 0.0335 seconds....16
13. Equivalent plastic strains in the 6 inch diameter pipe wall after an off-center impact with the tine....17
14. Deformed shapes and equivalent plastic strains for the twelve inch container from a top impact of a flat roof section....19
15. Deformed shapes and equivalent plastic strains for the six inch container from a top impact of a flat roof section....20
16. Load in the 6 inch and 12 inch pipes due to a top impact of a flat roof section....21
17. Energy absorbed by the 6 inch and 12 inch pipes due to a top impact of a flat roof section....21
18. Deformed shapes and equivalent plastic strains for the twelve inch container from a side impact of a flat roof section....22
19. Deformed shapes and equivalent plastic strains for the six inch container from a side impact of a flat roof section....23
20. Load in the 6 inch and 12 inch pipes due to a side impact of a flat roof section....24
21. Energy absorbed by the 6 inch and 12 inch pipes due to a side impact of a flat roof section....24
22. Opening between flange and lid for the 6 inch and 12 inch pipes due to a side impact of a flat roof section....25
23. Deformed shapes for the 12 inch container impacted on its side by the edge of a roof section....26
24. Plastic strain levels in the 12 inch container impacted on its side by the edge of a roof section....27
25. Deformed shapes for the 6 inch container impacted on its side by the edge of a roof section....28
26. Plastic strain levels in the 6 inch container impacted on its side by the edge of a roof section....29
27. Load in the 6 inch and 12 inch pipes due to a side impact of an edge of a roof section....30
28. Energy absorbed by the 6 inch and 12 inch pipes due to a side impact of an edge of a roof section....30

List of Tables

1. Material properties for stainless steel power law hardening plasticity models.....7
2. Material properties for linear hardening materials models.....8
3. Material properties for elastic materials model 8

Analysis in Support of Storage of Residues in the Pipe Overpack Container

1. Introduction

The disposition of the large back-log of plutonium residues at the Rocky Flats Environmental Technology Site (Rocky Flats) will require interim storage and subsequent shipment to a waste repository. Current plans call for disposal at the Waste Isolation Pilot Plant (WIPP) and the transportation to WIPP in the TRUPACT-II. The transportation phase will require the residues to be packaged in a container that is more robust than a standard 55-gallon waste drum. Rocky Flats has designed the Pipe Overpack Container to meet this need. This container is a standard 55 gallon drum with an internal cylindrical stainless steel can made from a pipe section and separated from the drum by impact limiting material. The use of this same waste packaging for interim on-site storage in non-hardened buildings is desirable.

To assure the safety of this package during storage, a series of tests and analyses have been performed subjecting the package to various hypothetical accident scenarios. The results of the tests are documented in a separate report (Ammerman, et al., 1997a). This report discusses the result of finite element modeling of other accident scenarios. One potential risk to the integrity of the Pipe Overpack Container during handling or storage is the puncture of the container by the tine of a forklift. To address this concern, this container has been analyzed to assess the damage potential of a forklift tine impacting the container. The forklift is assumed to be traveling at 10 mph with a weight of 12,550 pounds for these analyses. The container will also be assumed to be pinned against a rigid wall. The impacting position of the tine will be chosen to maximize damage of the inner pipe container. Other possible accident scenarios involve the collapse of the roof structure of the storage building. Three possible impact orientations of the roof onto the package are analyzed: a flat section of roof impacting the top of the container, a flat section of roof impacting the side of the container, and the edge of a section of roof impacting the side of the container. In all analyses the roof section is assumed to be rigid and traveling at constant velocity. The amount of energy absorbed by the package prior to failure is calculated. This allows the risk assessment for these types of accidents to determine the weight of a roof section necessary to cause the package to fail.

2. Background Information

The pipe overpack container is designed for interim storage and transport within a TRUPACT-II container of plutonium materials for disposal at the WIPP site. Two different inner pipe sections are used in this container. One has a 6 inch diameter pipe and the other uses a 12 inch diameter pipe section. Figure 1 shows a section through the center of both of the Pipe Overpack Containers.

The overpack drum packages consist of a standard 55 gallon drum outside shell, a heavy plastic liner, impact limiting material and a stainless steel inner cylinder. The standard 55 gallon drum is approximately 23 inches in diameter by 32 inches in length. The drum is made out of mild carbon steel with a nominal wall thickness of 0.055 inches. The plastic liner just inside of the steel drum is included in the design to meet shipping requirements. The impact limiting material consists of

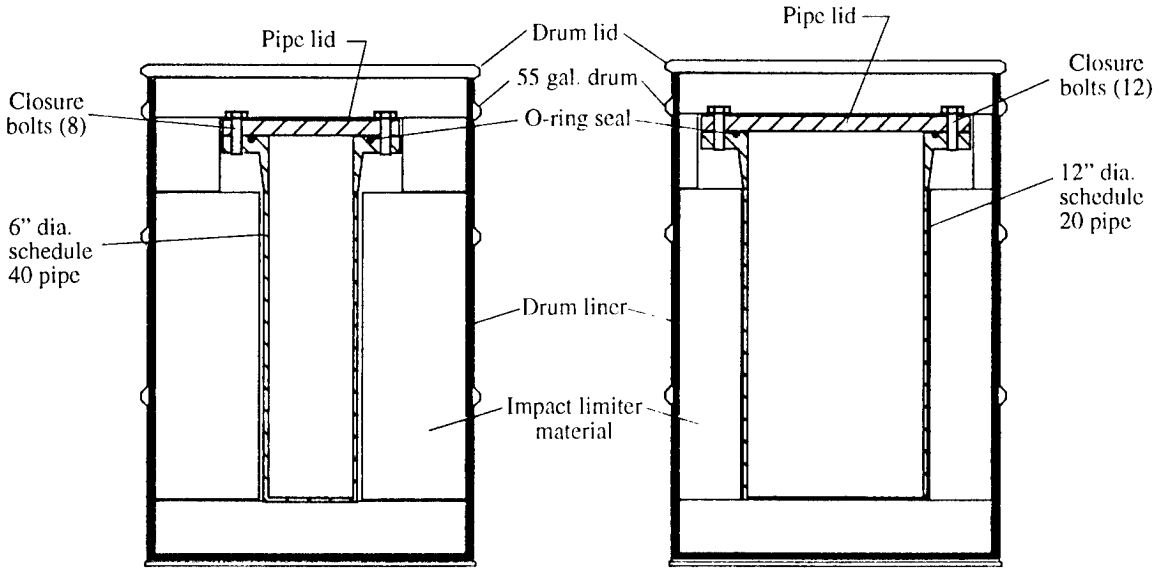

Figure 1: Diagram of the Pipe Overpack Container. The left figure is the 6" container and the right figure is the 12" container.

layers of Celotex® glued together. The inner package is either a stainless steel pipe section with a welded end plate or a formed cylinder with approximately a 0.25 inch wall thickness. The open end of the inner pipe is sealed with a welded flange and a bolted blind flange. Leak tightness is achieved with O-ring seals between the flanges.

3. Forklift Tine Analyses

The thin walled 55 gallon drum is a standard drum with a lid attached by a compression ring fastener. Three chines or upset rings in the wall are provided to increase the circular stiffness. The ability of the drum wall to resist the puncture and to slow the velocity of a tine will be minimal. The Celotex® will provide enough backing stiffness to force a tear in the drum wall rather than a collapse of the drum. The plastic liner which is included to meet shipping requirements will provide only negligible resistance to progress of the tine. For this reason it has been ignored in the analyses.

The Celotex® impact limiter material is a commonly used material in residential home construction. It is composed of compressed cane fibers and formed into sheets. The impact limiters in the containers are built up from several layers of the Celotex® sheet material glued together. The ability of the Celotex® material to slow the velocity of the tine will also be negligible due mainly to its weak strength when compared to the stiffness of the forklift tine.

The inner pipe container is either made from a short section of pipe with a plate welded to one end and a flange welded to the other or from a rolled cylinder with an integral end and a welded flange on the other end. Both methods of construction should yield similar products with regard to the

ability to resist a tine impact. The wall thickness are nominally 0.25 inches for the 12 inch diameter pipe section and 0.28 inches for the 6 inch diameter pipe.

The only two materials that will offer any significant resistance to the penetration of the tine are the outer drum wall and the inner stainless steel pipe section. The ability of the drum wall to resist the tine is dependent on the stiffness of the Celotex® backing material. The stiffer the backing material, the easier it is to induce a tear in the steel wall. The other extreme would be no backing; in that case the drum wall probably would not tear until it collapsed and contacted the inner pipe wall.

The inner pipe will be required to absorb the majority of the kinetic energy in the forklift if the container is to survive without leaking. The 12 inch diameter inner pipe will have the greatest chance of surviving without puncture due to its higher radius to wall thickness ratio. The larger radius to wall thickness ratio means the pipe wall is less stiff and can experience larger deformations without large membrane bending stresses when compared to the 6 inch pipe.

3.1. Finite element modeling

In order to accurately capture the time history and correctly account for the inertial effects, the nonlinear, transient dynamic computer program PRONTO3D (Taylor and Flanagan, 1992 and Attaway, 1993) code was used. The PRONTO3D code is an explicitly integrated code that steps through time, predicting the next time step conditions from the present conditions.

The stainless steel material in the inner pipe, where any failure will occur, was modeled with a realistic analytical material model based on a power law relationship (Stone, 1990) to represent the post yield plasticity of the material. All other materials were modeled with a bilinear elastic plastic material model. These materials include the outer steel drum, Celotex® impact limiter, the plywood which contributes little to the behavior of overpack, and the contents. The material properties used in the nonlinear dynamic analyses are shown in Tables 1, 2 and 3.

Table 1: Material properties for stainless steel power law hardening plasticity models

	304 Stainless Steel
Density	0.00074 lb-s^2-in^{-4}
Young's Modulus	28 x 10^6 psi
Poisson's Ratio	0.27
Yield Stress	28,000 psi
Hardening Constant	192,746
Hardening Exponent	0.748190
Luders Strain	0.0

Table 2: Material properties for linear hardening materials models

	Drum Wall	Celotex®	Tine	Contents
Density	0.00074 lb-s^2-in^{-4}	.000024 lb-s^2-in^{-4}	0.4697 lb-s^2-in^{-4}	.000024 lb-s^2-in^{-4}
Young's Modulus	28 x 10^6 psi	10,000 psi	30 x 10^6 psi	10,000 psi
Poisson's Ratio	0.27	0.05	0.3	0.2
Yield Strength	40,000 psi	50 psi	150,000 psi	25 psi
Hardening Modulus	10,000 psi	3,500 psi	10,000 psi	0.0 psi
Beta	0.0	0.5	1.0	0.0

Table 3: Material properties for elastic materials model

	Plywood
Density	0.00004 lb-s^2-in^{-4}
Young's Modulus	4,500 psi
Poisson's Ratio	0.2

The stainless steel material described in Table 1 is represented by an elastic plastic material model with a power law representation of the strain hardening. Before yielding stresses are reached the material is assumed to be elastic. After the elastic limit of the material is reached, the stress strain relationship can be represented by the power law relationship shown in Equation 1.

$$\sigma = \sigma_y + A(\varepsilon - L)^n \qquad \text{(EQ 1)}$$

where:

σ = Stress state
ε = Material strain
σ_y = Yield stress
L = Luder's strain
A = Hardening constant
n = Hardening exponent

The Luder's strain is the flat region of plasticity just after yield which is common in mild carbon steels. For the 304 stainless steel material used in the model the Luder's strain is negligible and has been set to zero.

The elastic-plastic material model used to model the tine, carbon steel drum, Celotex® and the contents is a bilinear model with an elastic region up to the yield stress limit and a linear hardening region after yield. Unloading proceeds along a line parallel to the elastic portion of the stress strain curve. The beta constant is a kinematic hardening term that becomes significant when load reversals exist. Very little load reversing is expected in these analyses so this term has minimal influence on the results.

The tine and the steel drum use typical values for high strength and mild carbon steels. The Celotex® parameters are based upon uniaxial test data of Celotex® samples. The Celotex® has a small initial yield strength followed by a relatively flat and long plasticity region. The contents were modeled as a very compliant material with a density similar to wood. To be conservative the contents material properties were chosen to contribute little to the stiffness of the inner cylinder.

The finite element model includes the outer drum, the Celotex® impact limiting material, the inner pipe container, the plywood in the base, the contents and the tine. The tine shown has an artificially very high density to account for the mass of the forklift. The tine also has a squared off end which should represent the worst case geometry of a tine concerning the ability of sharp corners on the tip to penetrate or tear the container materials. The outer drum wall and the inner pipe are modeled with 4-noded shell elements and the remainder of the model including both ends of the pipe are modeled with 8-noded solid hex elements. The shell elements are more computationally efficient for thin sections such as the drum wall while still maintaining the ability to accurately model bending and the in-plane membrane stresses. The finite element mesh is shown in Figure 2. Only half of the container was modeled to take advantage of the plane of symmetry present in the problem. Appropriate boundary conditions to prevent rotations and displacements across the plane of symmetry were incorporated into the model. In the figure, the drum and pipe walls which are modeled with shell elements will not appear to have any thickness. The thicknesses of these elements are included in the model data base and are used within the PRONTO3D code. The missing pieces of impact limiter in the top and bottom are in areas where little response is expected. They were left out to simplify the construction of the model.

The model of the tine assumed that the end of the tine was tapered on the top and bottom surfaces. The sides were flat and the end was squared off as viewed from above. The sharp corners at the tip of the tine are meant to be represent a worst case geometry. The sharp corners will help contribute to any tearing or penetration by inducing large strain concentrations in the materials at this location. The strain concentration effect of the sharp corner is reduced by the pipe elements finite size smearing any strain concentrations over the element. Most tines are rounded off to some degree and therefore would not create as large of strain concentrations as the one included in these analyses.

The boundary conditions for the model consisted of a rigid impact plane just to the left of the model and an initial velocity applied to the tine. The tine is constrained to travel only in a horizontal direction. The nodes in the plane of symmetry are constrained to stay in the plane but free to move in the other degrees of freedom.

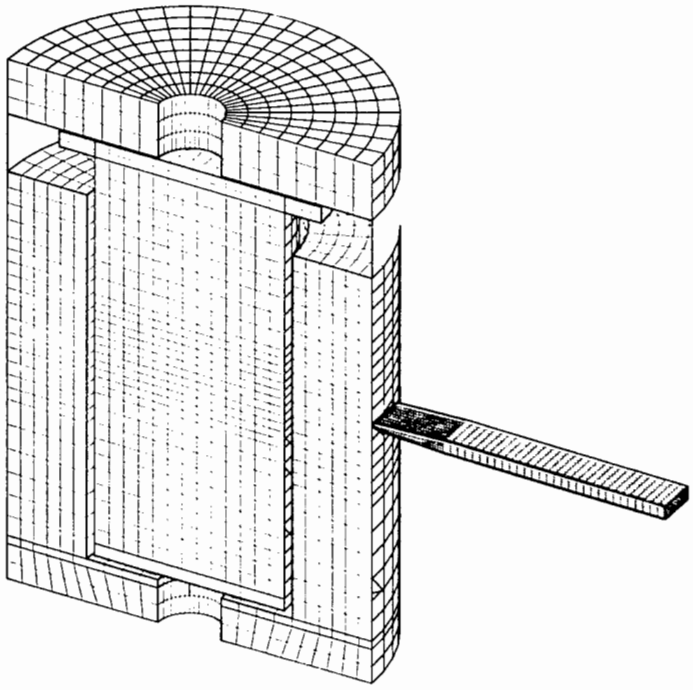

Figure 2: Finite element model of the Pipe Overpack Container with 12 inch inner pipe.

3.2. 12 inch Diameter Inner Container Results

The analysis was performed in two stages to both reduce the computation time and to reduce the errors associated with explicit integration schemes used over long time intervals. The first portion of the analysis was to determine the amount of kinetic energy taken out of the forklift due to the impact and penetration of the outer steel drum by the tine. The mesh for this analysis is shown in Figure 3. PRONTO3D has the capability to allow elements to fail and be removed from the computation when specified parameters are exceeded within the elements. When the elements fail they are disconnected from the parent material and do not contribute to the stiffness of the model for the remainder of the analysis. In this model the drum elements were allowed to fail at an equivalent plastic strain of 20%. Although mild carbon steel can achieve higher plastic strain levels in uniaxial tests, the plate elements used to model the drum will smear any localized strain concentrations. The 20% is more of a global strain limit than an absolute strain limit.

The tine is initially traveling at 10 mph or 176 inches/second in the horizontal direction. The deformed mesh is shown in Figure 4 at a time of 0.02 seconds. Figure 5 shows the outer drum shell after the failed elements are removed from the plot. After failure of the drum the tine is traveling at a velocity of approximately 9.4 mph or 166 inches/second. This indicates that the outer drum was relatively ineffective at slowing down the forklift, as anticipated.

The second portion of the analysis assumed that the Celotex® material did not slow the tine down any further. The tine velocity of 9.4 mph or 166 inches/second was applied directly to the inner

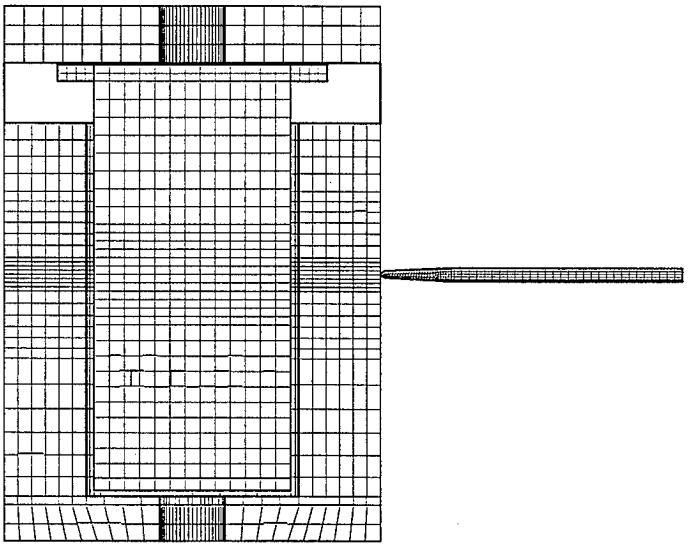

Figure 3: Finite element mesh of the tine impacting the outer drum wall.

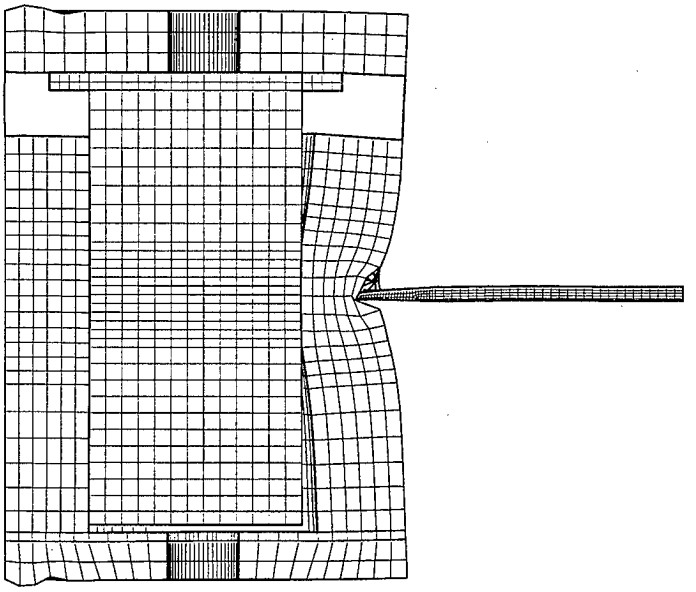

Figure 4: Mesh showing tine piercing the drum wall.

pipe wall. The mesh showing the initial configuration of the tine impact with the pipe wall is shown in Figure 6.

The elements in the wall of the pipe were assumed to fail when the equivalent plastic strain reached 80%. Again this is more of a global strain that does not include any strain concentrations that occur in areas smaller than the element size. The outer corner of the tip of the tine will create a significant strain concentration in the wall of the inner pipe as the deflection become large. Any puncture of the pipe will most likely initiate at this location.

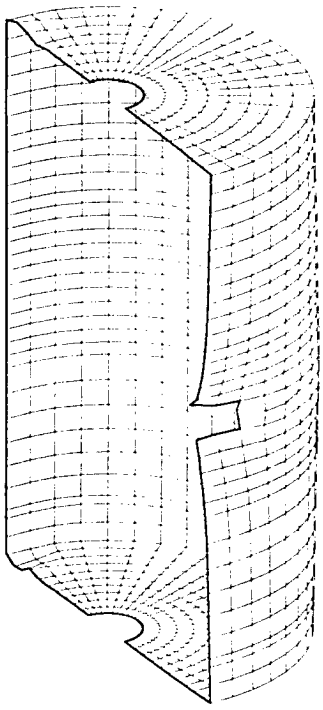

Figure 5: View of the drum wall with failed elements removed from the mesh.

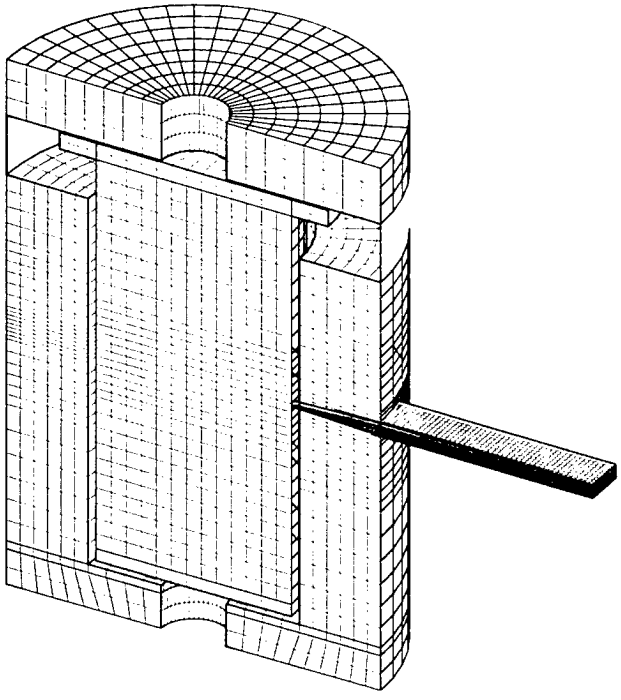

Figure 6: Mesh showing the position of the tine at the beginning of the second portion of the analysis.

The pipe was able to stop the tine as shown in Figure 7. In the figure the tine is shown rebounding away from the inner pipe. Figure 8 shows the equivalent plastic strains in the pipe wall. The strains in the wall exceed 80% with some of the elements having been removed from the analysis. The failure in the pipe wall occurred at the outer corner of the tine.

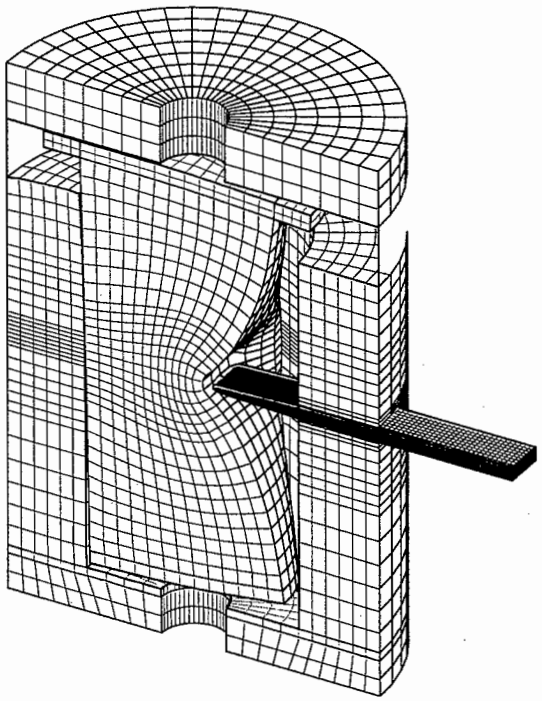

Figure 7: Deformed shape of the model after tine impact.

The strains in the inner pipe wall reached the 80% strain level at the very end of the tine penetration. In this analysis the pipe wall was very close to stopping the tine without failing. The ability of the pipe wall to resist the penetration of the tine will be very dependent on the failure strain limit of the stainless steel material and the geometry of the tine tip.

3.3. 6 inch Diameter Inner Container Results

The pipe impact conditions of the drum wall from the 12 inch diameter analysis was used again for the 6 inch diameter analysis. The tine was again given an initial velocity into the pipe wall of 9.4 mph or 166 inches/second. The mesh used in the analysis is shown in Figure 9.

When this analysis was run with the strain limit of 80% included in the pipe wall elements, the elements reached failure strain very early in the analysis. A large strain concentration at the outside tip of the tine caused the strains to exceed 80% while the tine was still moving quickly. The smaller pipe diameter combined with the higher thickness to radius ratio of the pipe contributed to the strain concentration. The 80% strain limit was turned off and the analysis was run again to see what strains would be attained and to see how much deformation would occur before the tine stopped. Figure 10 shows the deformation in the inner pipe when the tine has started rebounding.

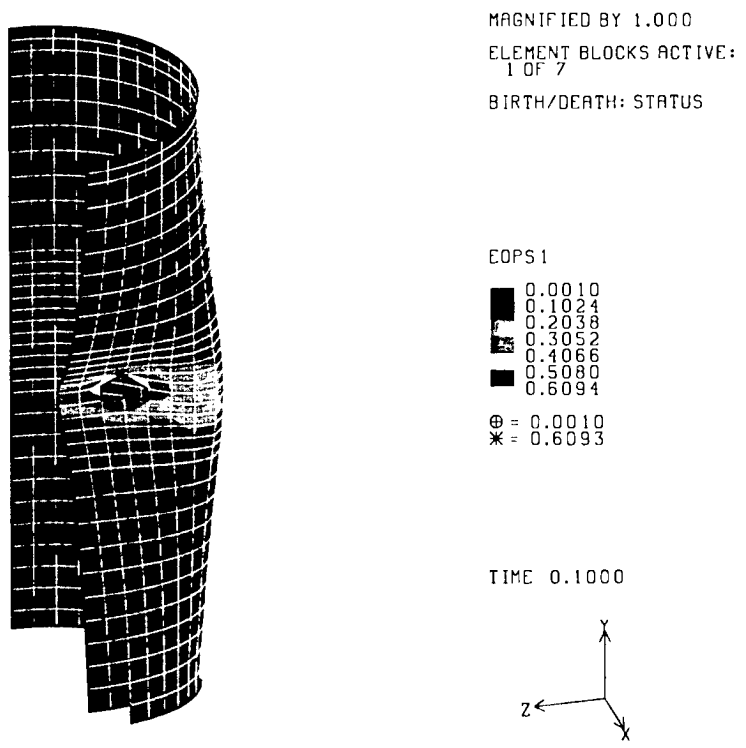

Figure 8: Equivalent plastic strain in the pipe wall after failed elements have been removed.

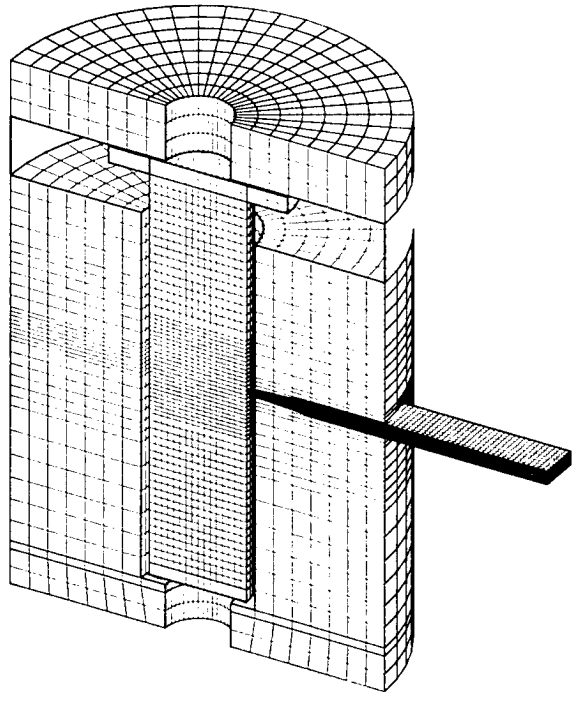

Figure 9: Mesh used in the analysis of the 6 inch pipe overpack container.

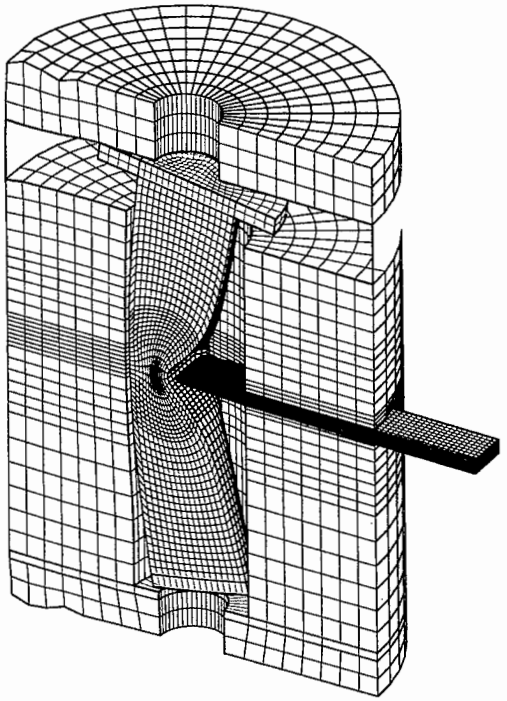

Figure 10: Deformed shape of the 6 inch pipe overpack container.

The strains in the pipe wall exceeded 120% for much of the analysis in the area near the tine outside tip impact location. The strains stayed very localized to this area throughout the analysis. This suggests that although the pipe wall would most likely tear open in the location, the tear would stay localized. Figure 11 shows the equivalent plastic strains in the inner pipe wall at the end of the impact.

The failure of the 6 inch diameter inner pipe is very dependent on the ductility of the pipe material and the shape and impact orientation of the tine. Less ductile material would increase the likelihood of a tearing failure. Also a sharp tine with a sharp corner in its outside corners could impose large strain concentrations under certain impact conditions.

Other possible orientations of impact between the tine and the inner drum could make the strain concentration at the corner of the tine tip greater than the symmetrical straight on impact. If the tine impacted off center such that the corner of the tine could gouge the pipe wall, the tearing of the wall could be more severe. Figure 12 shows the results of an impact where the tine impacts the cylinder at a distance of 0.5 inches from the pipe center. The velocity at impact of the tine was the same as previous analyses or 9.4 mph (166 inches/second). The rigid wall behind the cask was also included in the analysis.

Figure 12 shows that the inner pipe was dented initially and then moved laterally and rotated away from the tine. The ability of the container to move away from the tine kept the damage to the inner pipe to a minimum. Figure 13 shows the equivalent plastic strains in the inner pipe after the end of

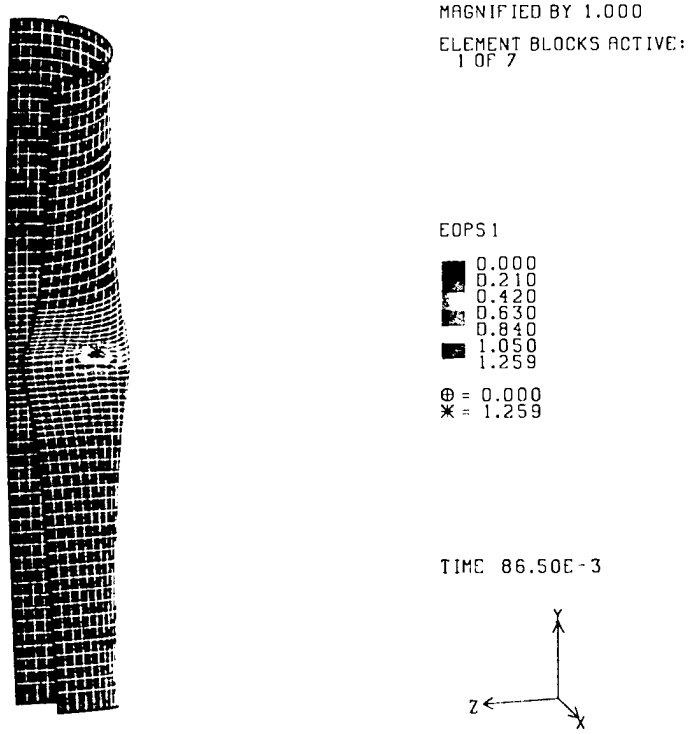

Figure 11: Equivalent plastic strains in the pipe wall after impact.

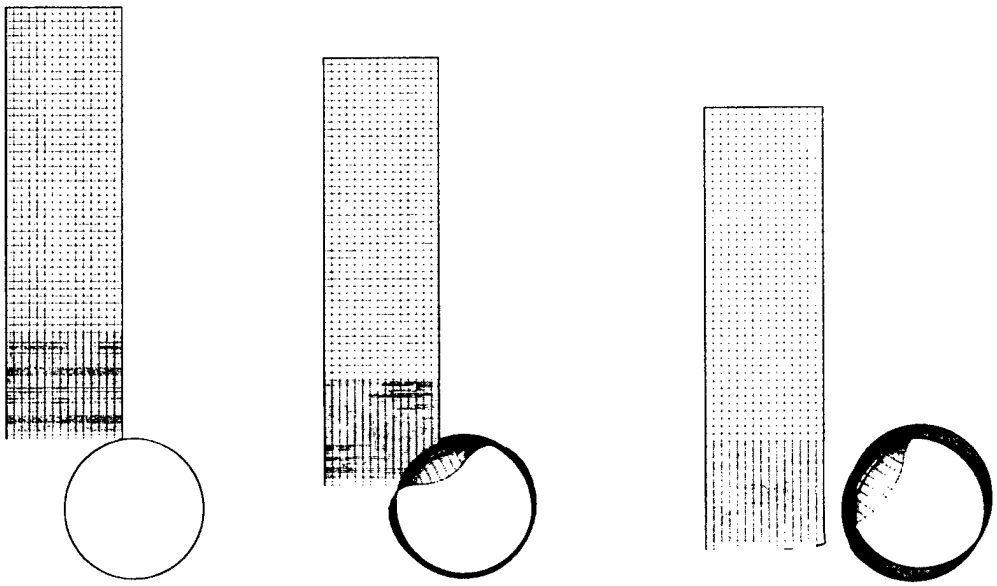

Figure 12: Overhead view of the impact between the tine and the 6 inch diameter inner cylinder at times of 0, 0.018, and 0.0335 seconds.

the analysis. The maximum strain of about 57% would indicate that the pipe would not fail from this impact with the tine. The ability of the cask to move away from the tine seems to be important in keeping the damage of the inner cylinder to a minimum.

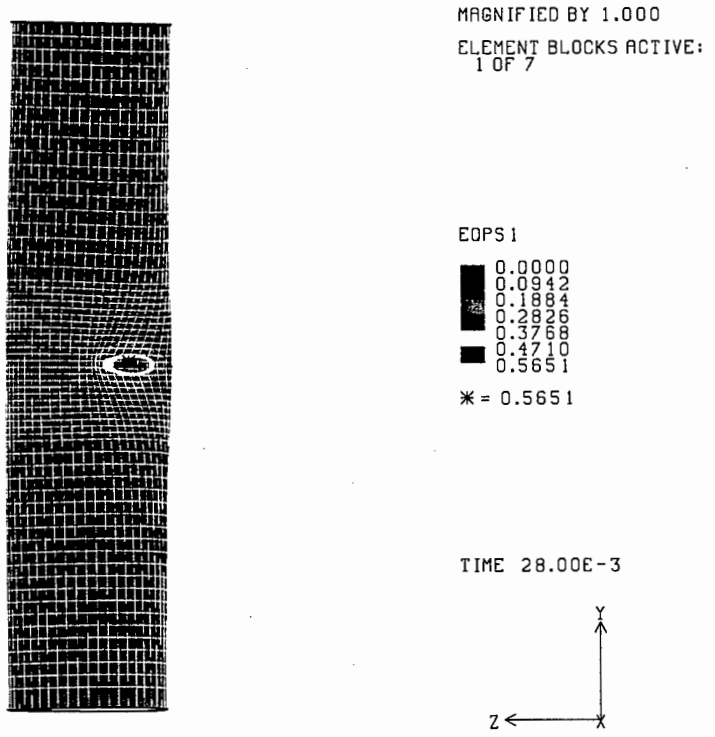

Figure 13: Equivalent plastic strains in the 6 inch diameter pipe wall after an off-center impact with the tine.

3.4. Summary of Forklift Tine Impact Analyses

The thin outer 55 gallon drum wall was not able to reduce the kinetic energy of the forklift by any appreciable amount. The initial velocity of 10 mph or 176 inches/second was reduced to only 9.4 mph or 166 inches/second. The Celotex® impact limiter was assumed to have no effect on the tine velocity. Thus the 9.4 mph or 166 inches/second forklift velocity was used as the impact velocity between the tine and the inner pipe cylinders.

Both the 12 inch and the 6 inch diameter inner pipes were capable of stopping the forklift without a total failure of the inner pipes. The pipes were bent significantly but remained relatively intact. The strain concentrations caused when the outside tip of the tine impacted the pipe were high enough to assume that local tearing of the pipe wall would occur at this location. The design of the tine used in these analyses had a squared off end which greatly contributed to the strain concentration.

A slightly off center impact was analyzed to see if this was a more severe impact than the symmetrical impact conditions. The ability of the pipe to move away from the tine was effective at keeping the strains in the internal pipe to below failure strain limits.

Even though this series of analyses assumed worst case scenarios, large failures are not predicted. The potential for some localized tearing is possible at the outside edge of the tine when the impact is straight on and symmetrical. Even with this unlikely impact condition, the predicted failure stayed localized and did not spread into a large failure. The ability of the pipe to move away from the tine in the off center impact indicates the importance of the rigid wall constraint behind the cask. Simply allowing the pipe to move laterally away from the tine was enough to significantly reduce the damage to the inner pipe.

4. Roof Collapse Analyses

During the storage of residues in Pipe Overpack Containers in an unhardened structure the possibility exists for the structure to collapse due to high winds, heavy snow loads, or earthquake. If this happens, the roof of the structure can impact the containers stored there. The ability for this type of accident to damage the Pipe Overpack Containers has been assessed using the finite element method. For all of the analyses the containers are assumed to be resting on a rigid surface and a rigid section of roof impacts the container. To estimate the amount of energy absorbed by the containers prior to failure a constant velocity, elastic mass representing the roof section is impacted onto the container being analyzed. This is esentially an infinite mass assumption (since the mass of the impacting roof section is not known), as the kinetic energy of the impacting mass does not change as energy is absorbed by the crushing container. Three impact orientations are considered for each of the 6 inch container and 12 inch container. In the first orientation the flat roof is assumed to impact the container on its top. This is the most likely orientation, as the containers are stored vertically. The second orientation analyzed is a flat roof section impacting the side of the container. This orientation can occur if the container tips over prior to roof impact. The final orientation analyzed is for the edge of a roof section impacting the side of the container. This can occur if there is a partial roof failure and the roof section rotates prior to impacting the containers. For all of the calculations the energy absorbed by the Celotex® and drum is ignored, and only the energy absorbed by the inner pipe container is calculated. For the top and side impact orientations the amount of energy absorbed by the Celotex® and drum can be estimated based upon results from tests performed on these containers. In the top impact scenario, the results of the dynamic crush tests performed indicated little or no plasticity within the inner pipe container (Ammerman et al., 1997a). This test involves an impact of a 500 kg plate impacting the container at a velocity of 13.4 m/s. The amount of kinetic energy in this impact is 400,000 inch-pounds. This amount of energy can be added to the values calculated below to get total energy absorbed. For the side impact by the flat roof section the test of the Pipe Overpack Containers inside the TRUPACT-II ICV can be used to estimate the amount of energy absorbed by the Celotex® and drum (Ammerman et al., 1997b). In this test a stack of three containers was impacted onto its side at a velocity of 13.4 m/s. The bottom container in this stack had the weight of two other containers compressing it. The weight of two loaded 12 inch Pipe Overpack Containers is about 1080 pounds, so the energy absorbed by the bottom container is at least 384,000 inch-pounds. For the 6 inch containers the weight of the packages crushing them is less, but the amount of energy they are able to absorb is higher, so assuming the Celotex® and drum for this container can also absorb 384,000 inch-pounds of energy is conservative. For the impact by the edge of the roof section the amount of Celotex® crushed is small and the energy absorbed by it will be negligible. For all of the analyses performed the finite element models of the pipes were similar to those used for the forklift tine puncture analyses. The material models and codes used were also the same.

4.1. Top Impact Results

The deformations and strains produced for the top impact case with the 12 inch diameter pipe are shown in Figure 14. The deformations and strains produced for the top impact case with the 6 inch diameter pipe are shown in Figure 15. Figure 16 shows the load applied to each pipe as a function of axial shortening and Figure 17 shows the energy absorbed by each pipe as a function of axial shortening. In both figures the point of assumed failure is shown by horizontal and vertical lines. Failure was assumed to occur when the buckle in the pipe section collapsed against itself. For the 12 inch pipe, the maximum load is about 420,000 pounds and the absorbed energy at failure is about 1,550,000 inch-pounds. For the 6 inch pipe the maximum load and failure energy are 400,000 pounds and 1,400,000 inch-pounds.

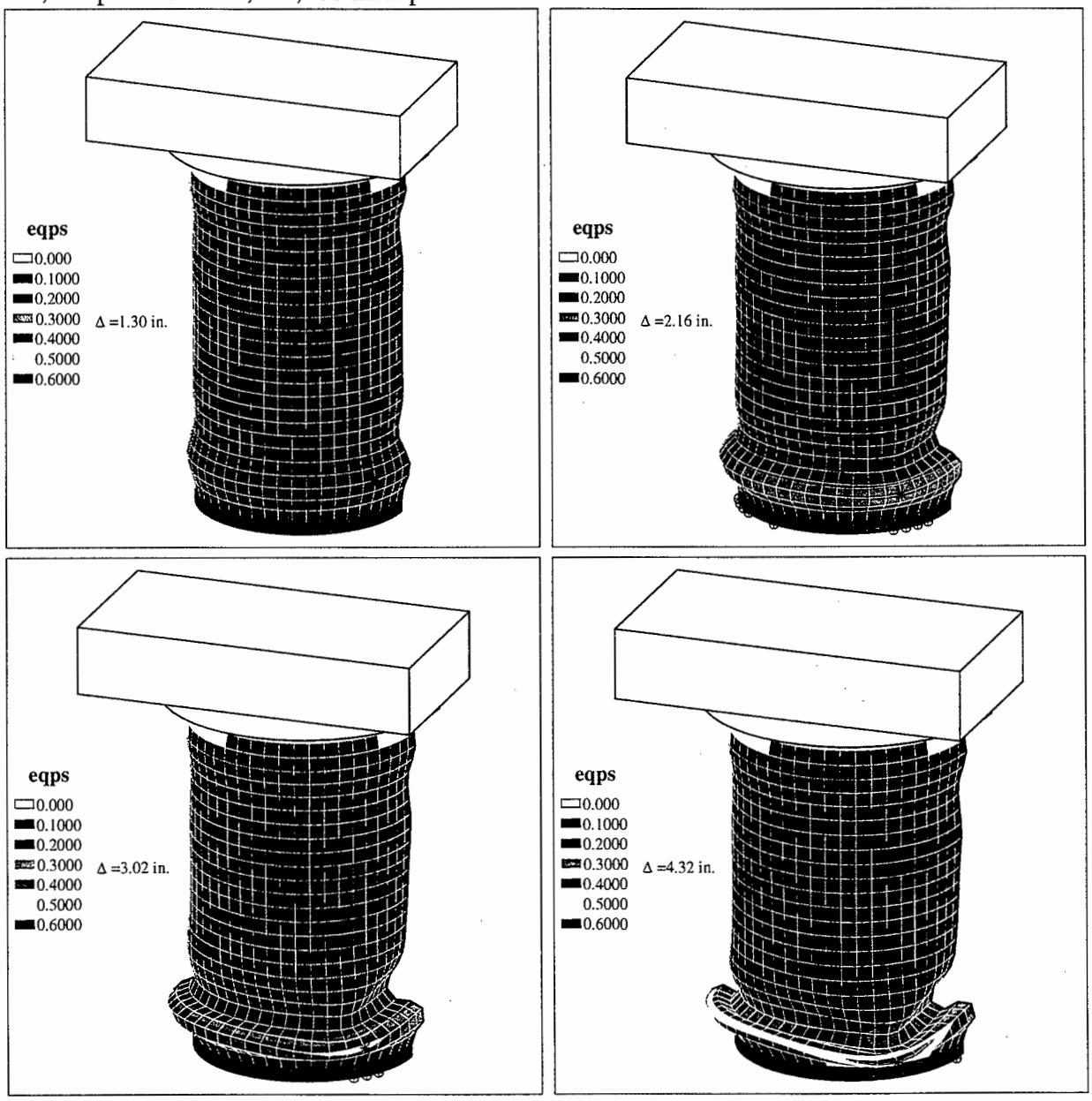

Figure 14: Deformed shapes and equivalent plastic strains for the twelve inch container from a top impact of a flat roof section.

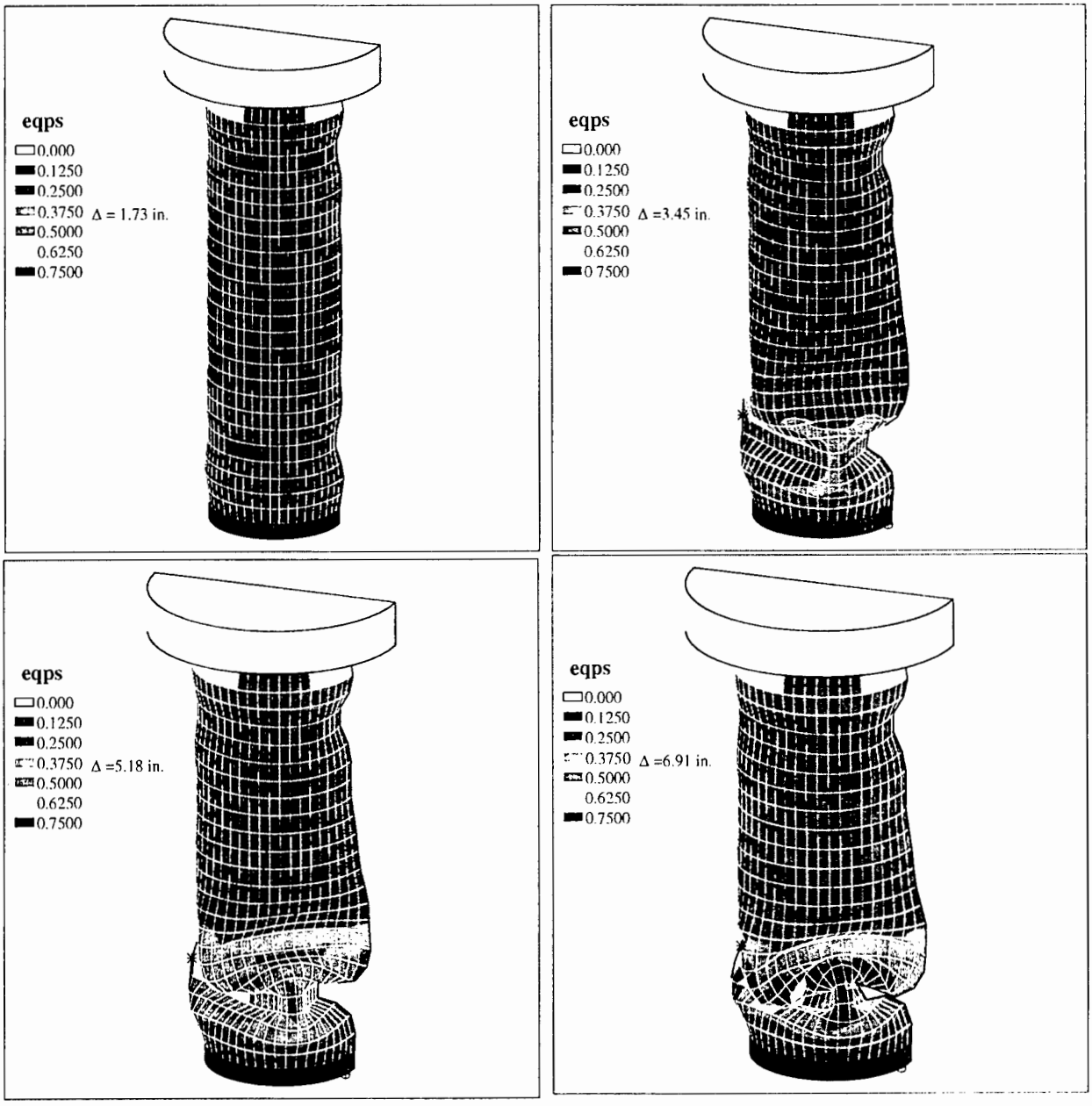

Figure 15: Deformed shapes and equivalent plastic strains for the six inch container from a top impact of a flat roof section.

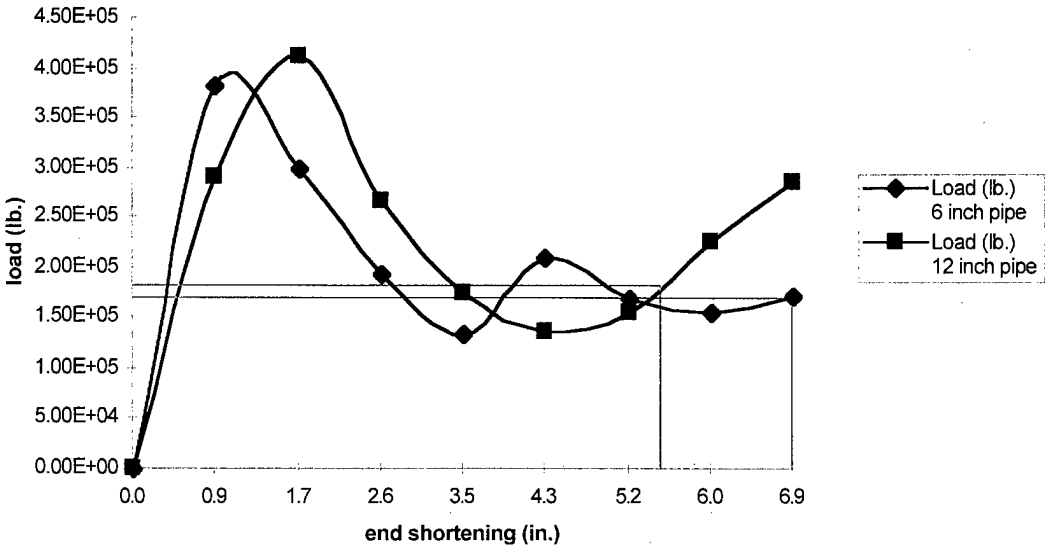

Figure 16: Load in the 6 inch and 12 inch pipes due to a top impact of a flat roof section.

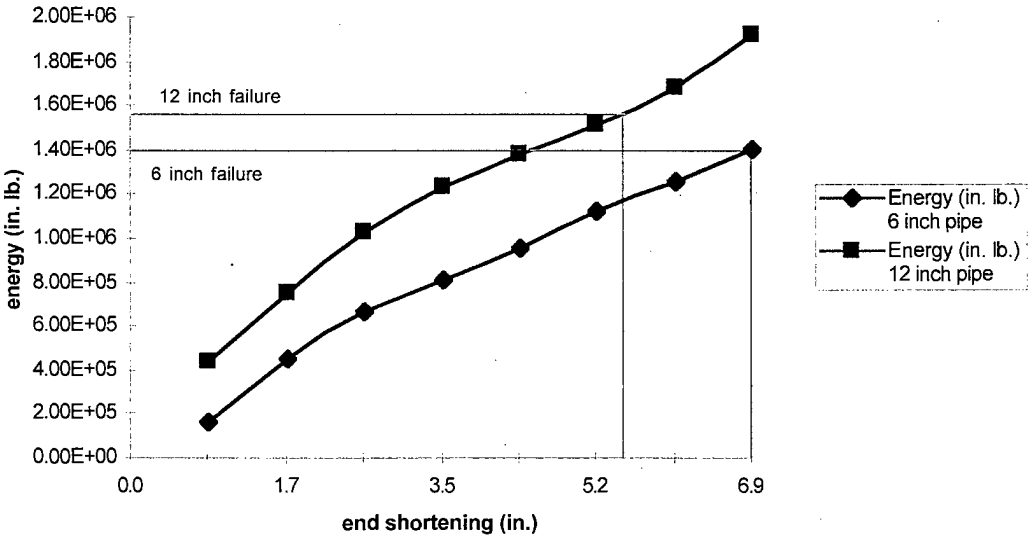

Figure 17: Energy absorbed by the 6 inch and 12 inch pipes due to a top impact of a flat roof section.

4.2. Side Impact Results

The deformations and strains produced for the side impact case with the 12 inch diameter pipe are shown in Figure 18. The deformations and strains produced for the side impact case with the 6 inch diameter pipe are shown in Figure 19. Figure 20 shows the load applied to each pipe as a function of diametrical shortening, Figure 21 shows the energy absorbed by each pipe as a function of diametrical shortening, and Figure 22 shows the opening between the flange and lid as a function of diametrical shortening. In these figures the point of assumed failure is shown by horizontal and vertical lines. Failure was assumed to occur when the gap between the lid and the flange was more than 0.06 inches. For the 12 inch pipe this occurs at a load of about 740,000 pounds and an

absorbed energy of about 1,500,000 inch-pounds. For the 6 inch pipe the failure load and energy are 630,000 pounds and 800,000 inch-pounds.

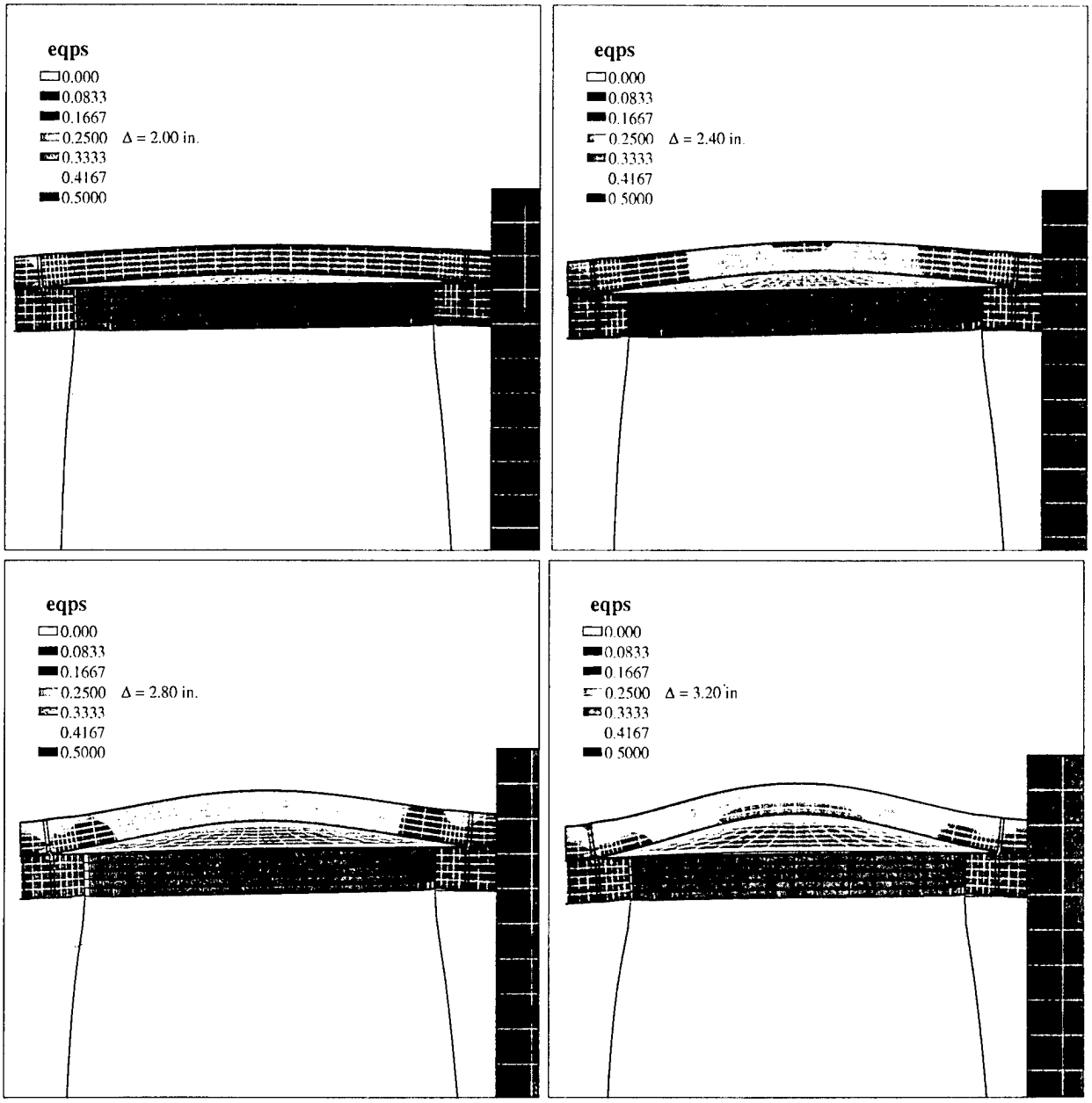

Figure 18: Deformed shapes and equivalent plastic strains for the twelve inch container from a side impact of a flat roof section.

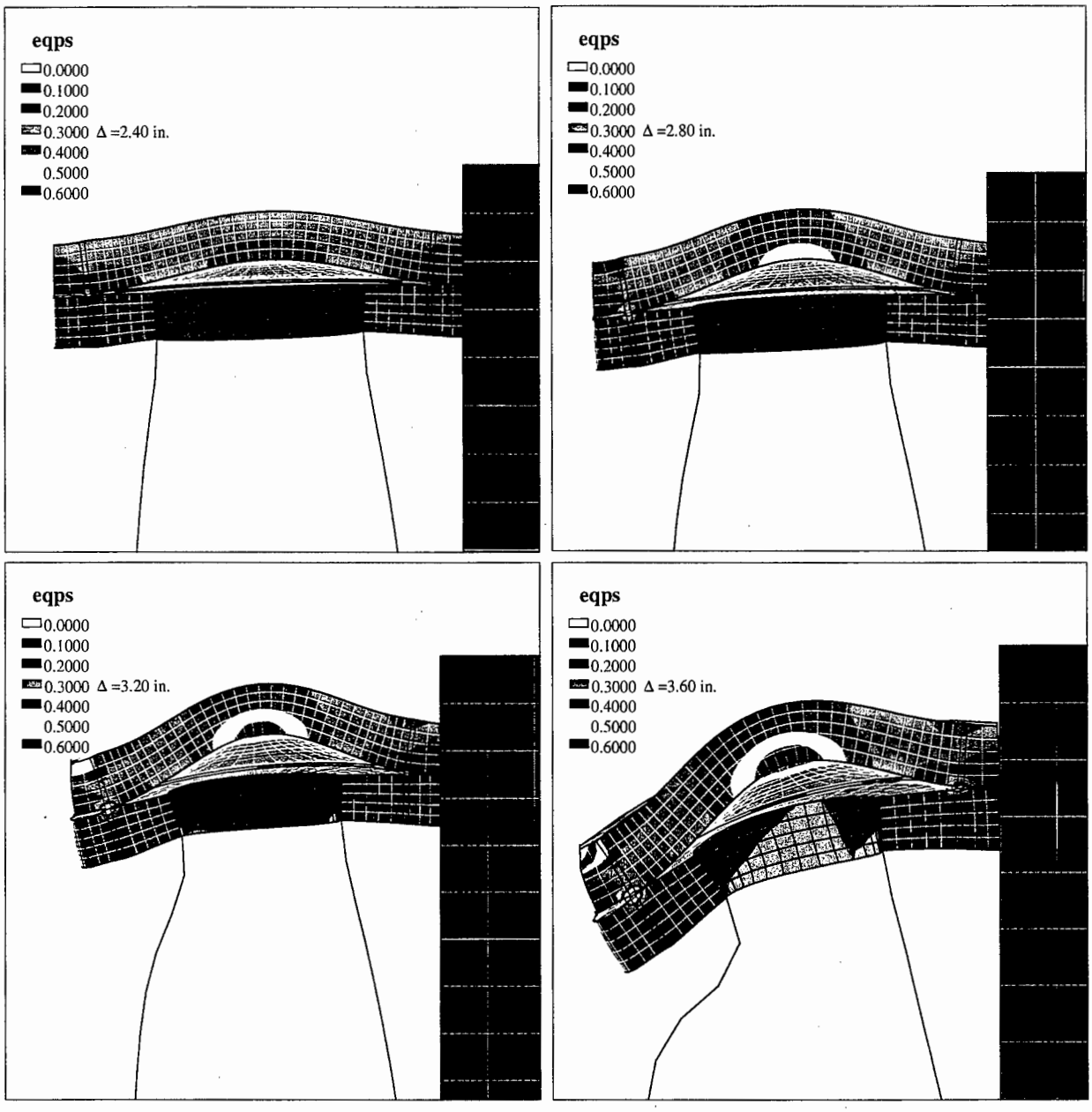

Figure 19: Deformed shapes and equivalent plastic strains for the six inch container from a side impact of a flat roof section.

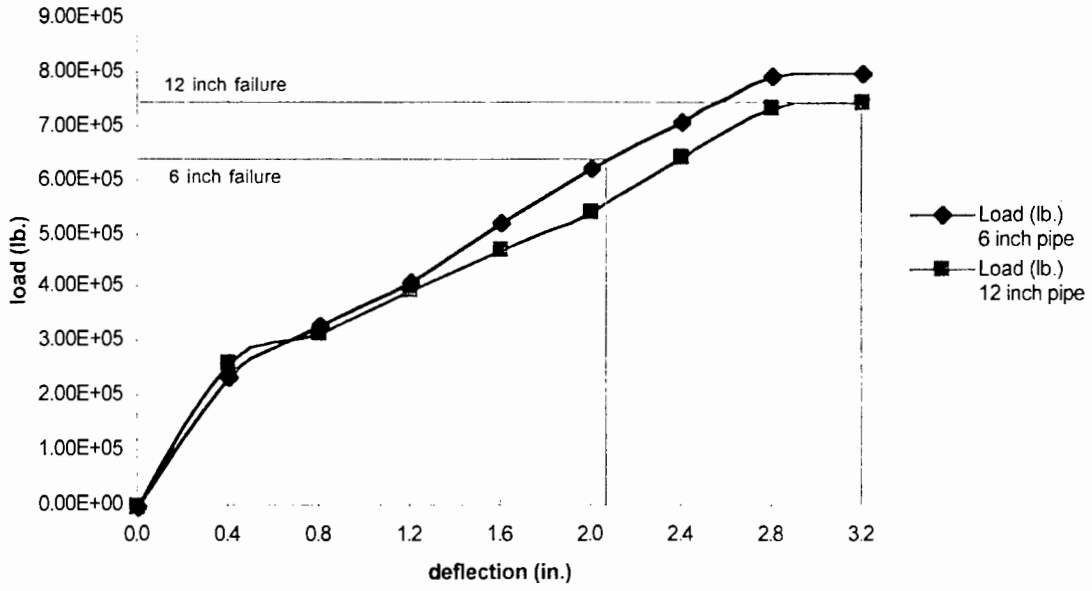

Figure 20: Load in the 6 inch and 12 inch pipes due to a side impact of a flat roof section.

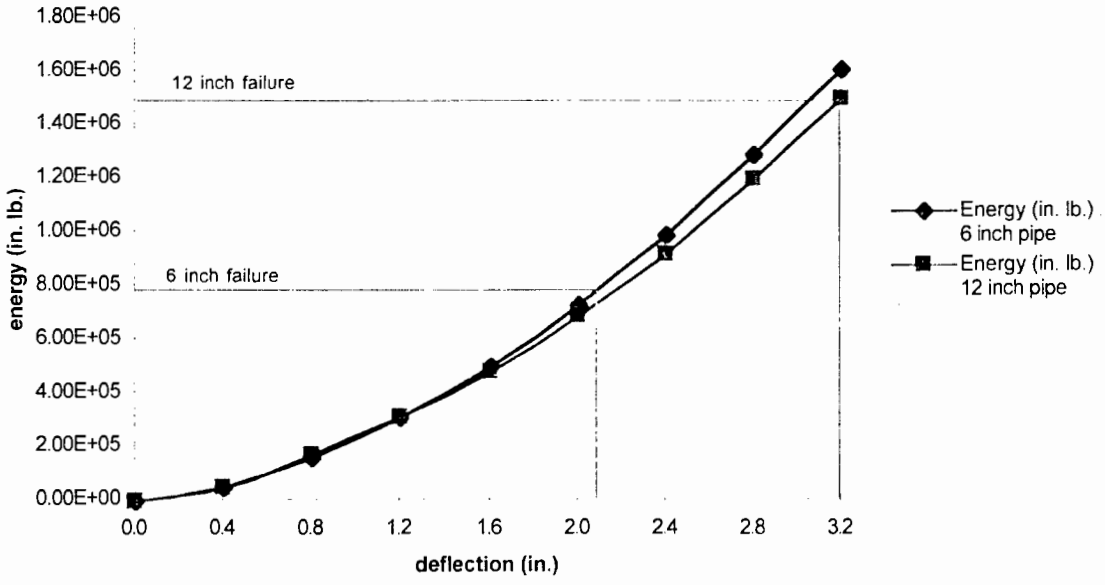

Figure 21: Energy absorbed by the 6 inch and 12 inch pipes due to a side impact of a flat roof section.

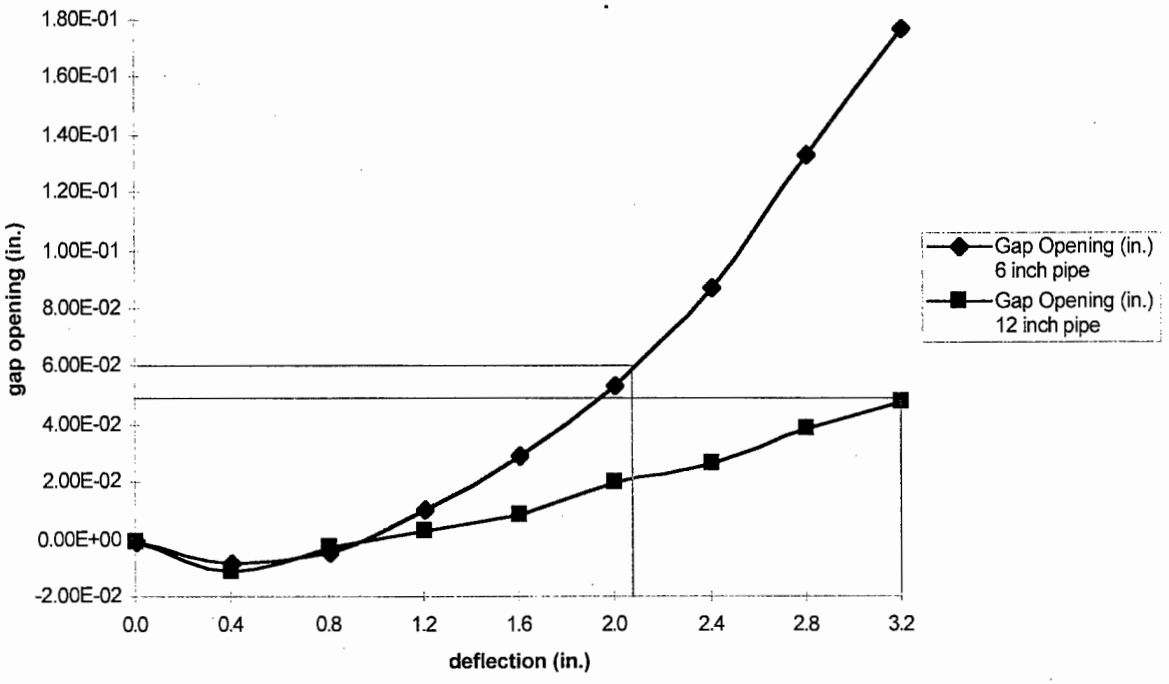

Figure 22: Opening between flange and lid for the 6 inch and 12 inch pipes due to a side impact of a flat roof section.

4.3. Edge Impact Results

The deformations produced during the side impact by the roof edge with the 12 inch diameter pipe are shown in Figure 23. The plastic strain level in the wall of the pipe is shown in Figure 24. The deformations produced during the side impact by the roof edge with the 6 inch diameter pipe are shown in Figure 25. The plastic strain level in the wall of the pipe is shown in Figure 26. Figure 27 shows the load applied to each pipe as a function of roof penetration distance and Figure 28 shows the energy absorbed by each pipe as a function of roof penetration distance. In both of these last two figures the point of assumed failure is shown by horizontal and vertical lines. Failure was assumed to occur when the maximum plastic strain in the pipe wall reached 60%. For the 12 inch pipe this occurs at a load of about 94,000 pounds and an absorbed energy of about 142,000 inch-pounds. For the 6 inch pipe the failure load and energy are 79,000 pounds and 178,000 inch-pounds.

4.4. Summary of Roof Collapse Analyses

These analyses indicate the amount of energy a single Pipe Overpack Container is able to absorb prior to failure in several orientations. In a real accident it is possible that more than one container will be impacted by the collapsing roof structure, and the total energy absorbed is equal to the energy absorbed by each package times the number of packages impacted. The amount of energy absorbed by a single package gives an indication of how massive of a roof section can fall from a given height and impact the package without causing package failure. For example, the 1,400,000 inch-pounds of energy absorbed by the 6-inch container in an end impact orientation plus the 400,000 inch pounds absorbed by the drum and Celotex® in this orientation, implies that this package would not fail if impacted by a 7500 pound roof section falling from 20 feet. For a four

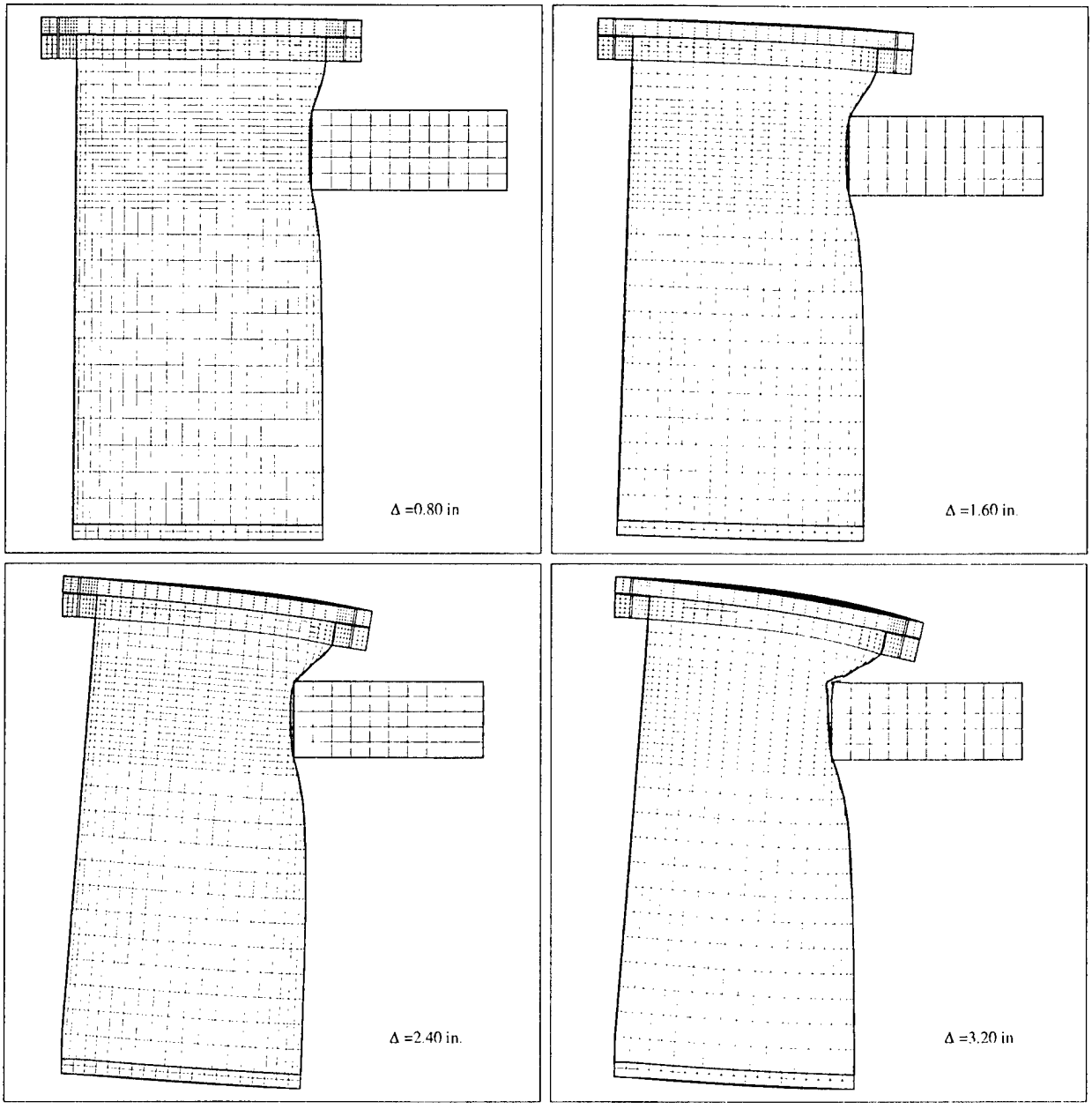

Figure 23: Deformed shapes for the 12 inch container impacted on its side by the edge of a roof section.

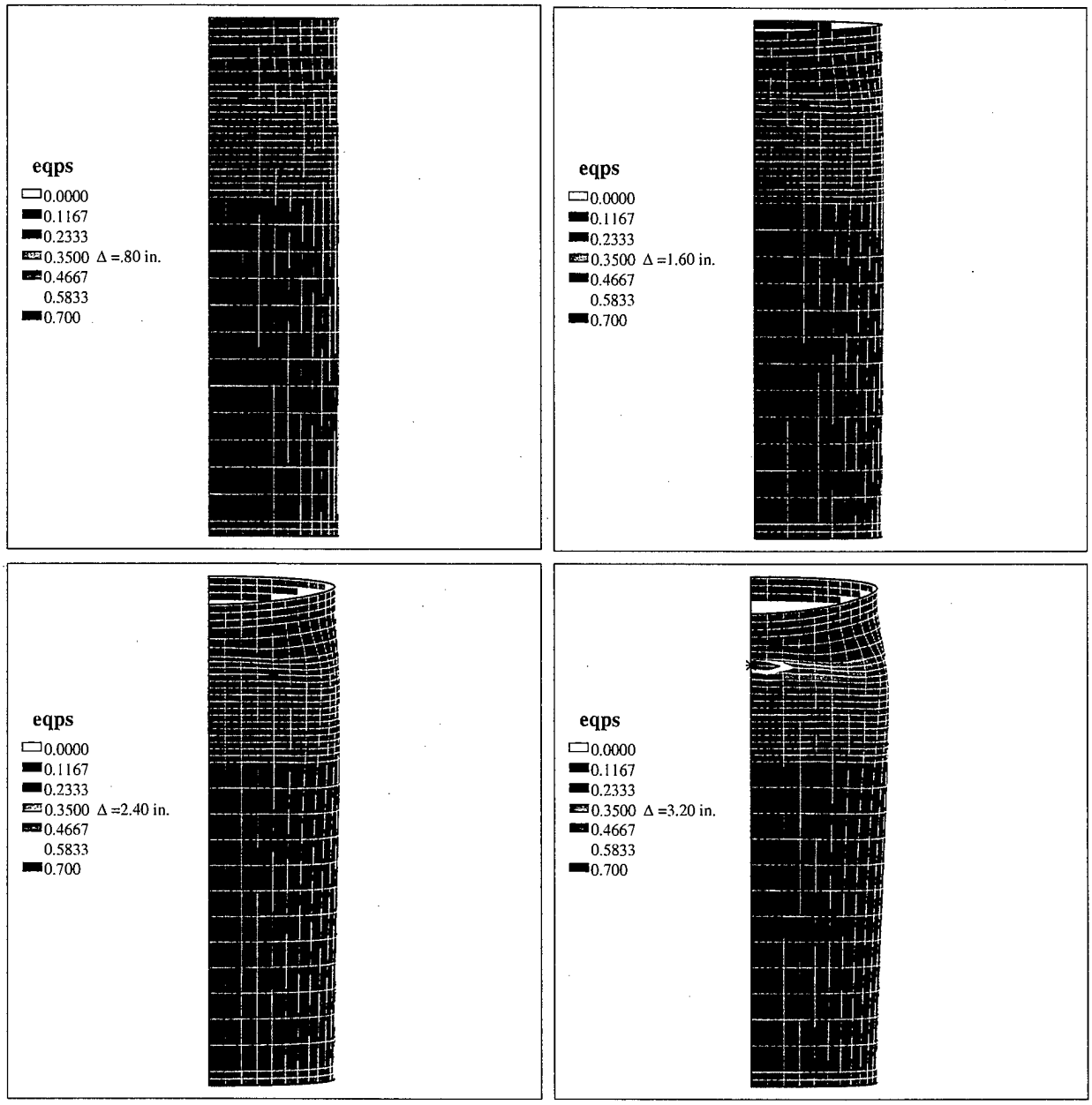

Figure 24: Plastic strain levels in the 12 inch container impacted on its side by the edge of a roof section.

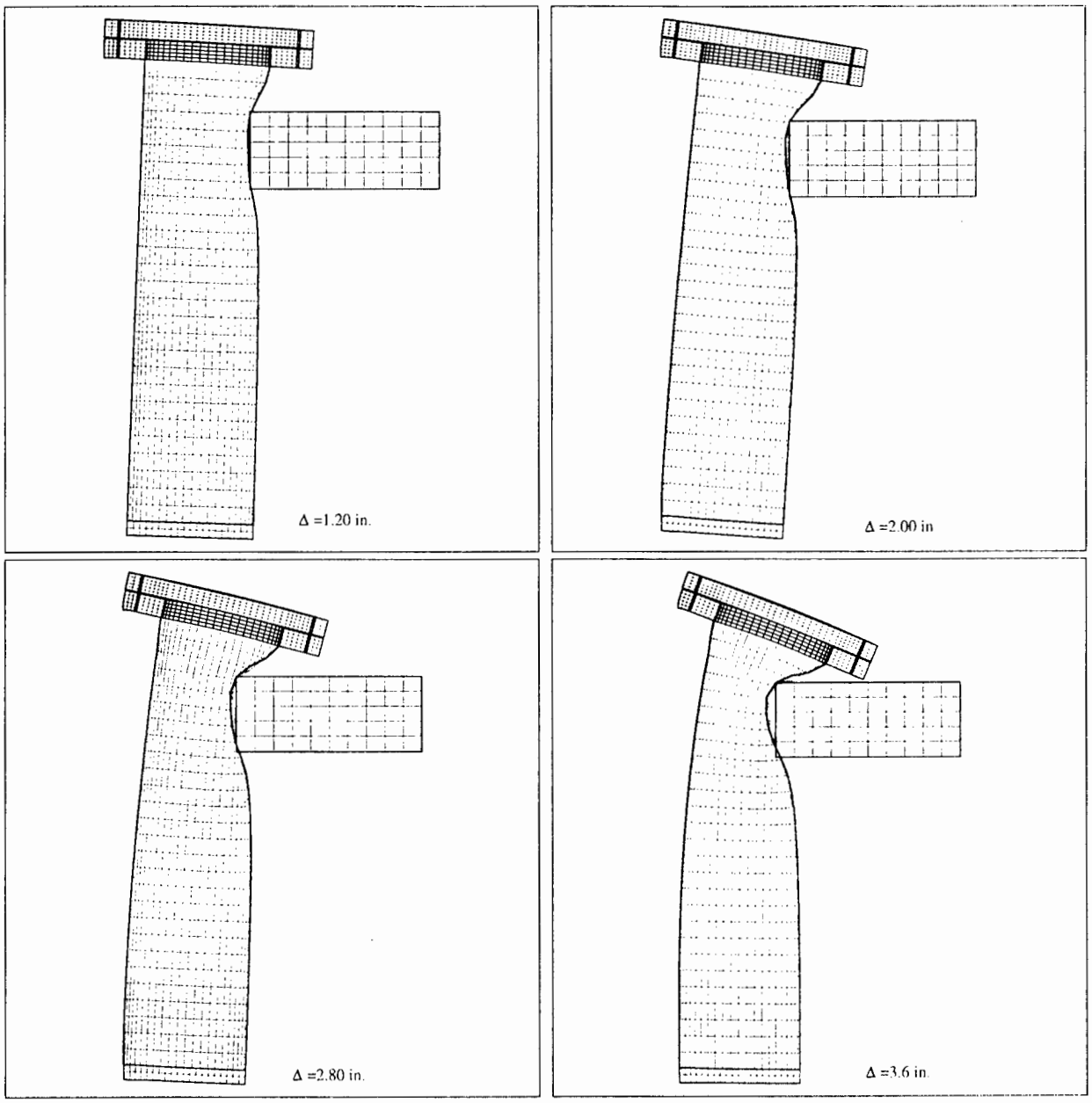

Figure 25: Deformed shapes for the 6 inch container impacted on its side by the edge of a roof section.

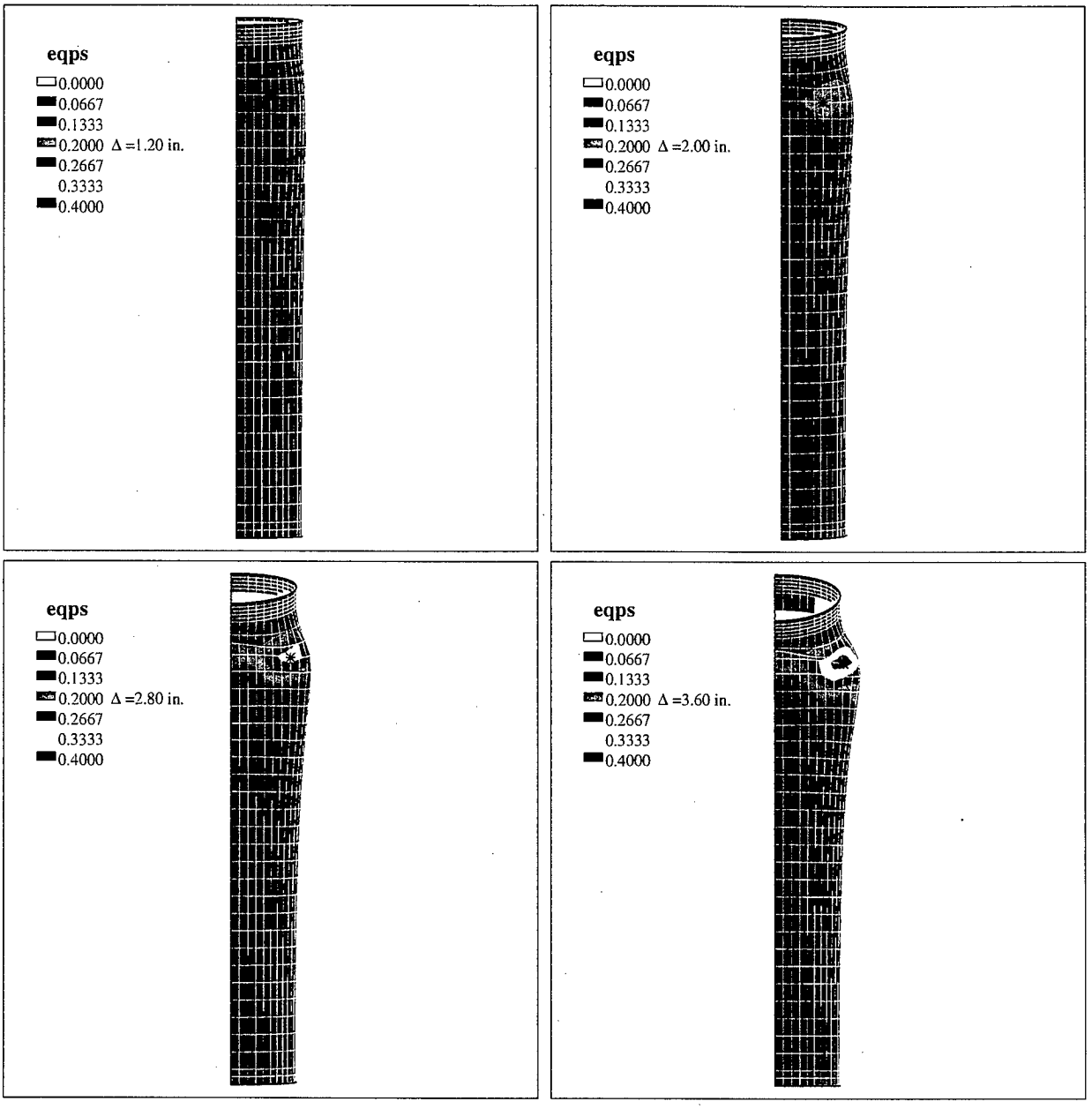

Figure 26: Plastic strain levels in the 6 inch container impacted on its side by the edge of a roof section.

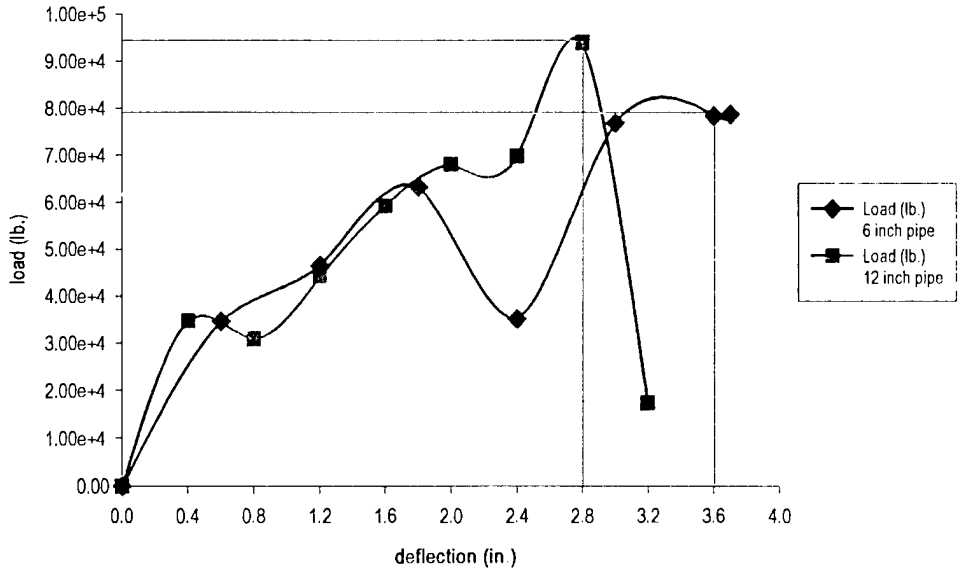

Figure 27: Load in the 6 inch and 12 inch pipes due to a side impact of an edge of a roof section.

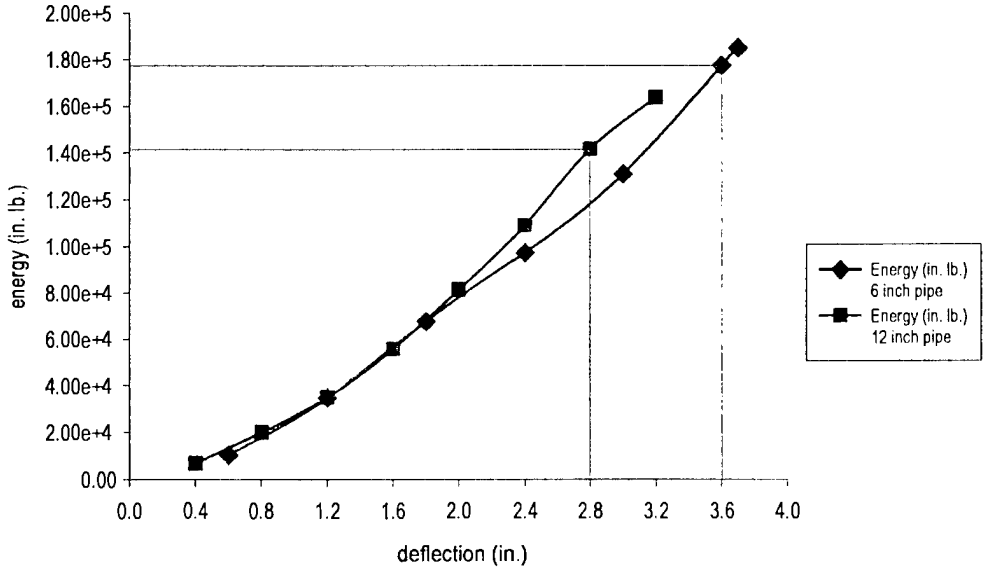

Figure 28: Energy absorbed by the 6 inch and 12 inch pipes due to a side impact of an edge of a roof section.

inch thick reinforced concrete slab this equates to a section more than 12 feet square. Even for impact of an edge of a roof section onto the side of the 12-inch container the 142,000 inch-pounds of absorbed energy is equal to a 590 pound roof section falling from 20 feet. For a 4 inch thick roof slab this weight is equal to about a 3.5 feet square section.

5. Conclusions

The ability of the Pipe Overpack Container to contain its contents following several severe accident scenarios that could occur during on-site storage of the containers in unhardened facilities has been investigated using the finite element technique. For the forklift tine impact the analyses show that even with very conservative assumptions the tine will barely (if at all) penetrate the 12-inch container. For the 6-inch container if it is prevented from moving away from the impact the tine will completely penetrate one side of the container, but not the other side. If the impact is off-center the container will translate without being penetrated. For the roof collapse analyses the amount of energy required to cause failure of the containers in three different orientations has been calculated. The minimum energy required to produce failure when the flat side of the roof impacts the container is equivalent to a 12 feet square section of 4 inch thick concrete roof structure falling from a height of 20 feet. Even in the more damaging case of the edge of a roof section hitting a container in the most vulnerable location and orientation the energy required to produce failure is equivalent to a 3.5 feet square section of roof falling from 20 feet.

6. References

Ammerman, D. J., Bobbe, J. G., and Arviso, M., 1997a, "Testing in Support of On-Site Storage of Residues in the Pipe Overpack Container", SAND97-0368, Sandia National Laboratories, Albuquerque, NM.

Ammerman, D. J., Bobbe, J. G., Arviso, M., and Bronowski, D. R., 1997b, "Testing in Support of Transportation of Residues in the Pipe Overpack Container", SAND97-0716, Sandia National Laboratories, Albuquerque, NM.

Attaway, S. W., 1992, "Update of PRONTO2D and PRONTO3D Transient Solid Dynamics Program," SAND90-0102, Sandia National Laboratories, Albuquerque, NM.

Stone, C. M., Wellman, G. W., and Krieg, R. D., 1990 "A Vectorized Elastic-Plastic Power Law Hardening Material Model Including Luders Strain," SAND90-0153, Sandia National Laboratories, Albuquerque, NM.

Taylor, L. M., and Flanagan, D. P., 1987 "PRONTO3D: A Three-dimensional Transient Solid Dynamics Program," SAND87-1912, Sandia National Laboratories, Albuquerque, NM.

Distribution List

No. of
Copies

1 Kevin J. Keenan
US Department of Energy
Rocky Flats Field Office
P.O. Box 928
Golden, CO 80402-0928

1 Rick Geinitz
SNM Programs
Safe Sites of Colorado, For US DOE
Rocky Flats Environmental Technology Site
Building 750
P.O. Box 464
Golden, CO 80402-0464

5 Mike Rivera
LATA/SSOC
Rocky Flats Environmental Technology Site
P.O. Box 464
Bldg. 111
Golden, CO 80402-0464

1 Elizabeth Conrad
LATA/SSOC
Rocky Flats Environmental Technology Site
P.O. Box 464
Bldg. 111
Golden, CO 80402-0464

3 Don Thorp
Safe Sites of Colorado, For US DOE
Rocky Flats Environmental Technology Site
P.O. Box 464
Trailer 115A
Golden, CO 80402-0464

1 Don Dustin
Safe Sites of Colorado, For US DOE
Rocky Flats Environmental Technology Site
P.O. Box 464
Trailer 115A
Golden, CO 80402-0464

1 Kathy London
Safe Sites of Colorado, For US DOE
Rocky Flats Environmental Technology Site
P.O. Box 464
Trailer 115A
Golden, CO 80402-0464

Internal Distribution

No. of
Copies

10	MS0715	TTC Library
10	MS0717	D. J. Ammerman, 6342
1	MS0717	H. D. Radloff, 6342
1	MS0717	G. F. Hohnstreiter, 6342
1	MS0724	J. B. Woodard, 6000
1	MS0744	J. S. Ludwigsen, 6403
1	MS0744	D. L. Berry, 6403
1	MS0766	D. E. Ellis, 6300
2	MS0899	Technical Library, 4916
1	MS9018	Central Technical Files, 8940-2
2	MS0619	Review & Approval Desk, 12690 For DOE/OSTI

Report Number (14) SAND--98-1003

Publ. Date (11) 199804
Sponsor Code (18) DOE/DP, XF
JC Category (19) UC-722, DOE/ER

ph

DOE